KINETIC ANALYSIS AND MODELING OF HEMP SEED OIL METHANOLYSIS OVER QUICKLIME

Milan D. Kostić*, Biljana S. Đorđević, Milica Z. Petković, Marija R. Miladinović, Olivera S. Stamenković

Faculty of Technology, University of Niš, Leskovac, Serbia

(ORIGINAL SCIENTIFIC PAPER)
UDC: 662.756.3:677.12
DOI: 10.5937/savteh2502059K

Hemp (*Cannabis sativa* L.) is a versatile crop used across multiple industries, and its seed oil has potential application as a renewable raw material for biodiesel production. This study investigates the kinetics of biodiesel production via quicklime-catalyzed methanolysis of hemp seed oil (HSO). Owing to the moderately high concentration of free fatty acids, HSO was first subjected to esterification. The methanolysis of the esterified HSO was performed at methanol-to-HSO molar ratios of 6:1, 9:1, and 12:1, with quicklime amounts of 3%, 5%, and 7% of HSO mass, at 60 °C under atmospheric pressure. The kinetics of the methanolysis reaction was evaluated using two different kinetic models: a pseudo-first order model and a model involving a changing reaction mechanism coupled with triacylglycerol (TAG) mass transfer limitations. The pseudo-first order model effectively described the reaction kinetics within two distinct regimes, initially controlled by TAG mass transfer, followed by a chemical reaction-controlled regime. The second model provided a continuous description of the reaction kinetics over the whole reaction course. The volumetric TAG mass transfer coefficient and the parameter defining the affinity of TAG to the active sites of the catalyst were found to be independent of methanol concentration but increased with catalyst amount. Both models yielded the same apparent reaction rate constant (0.155 min^{-1}) and demonstrated very good agreement with experimental TAG conversion degree data (*MRPD* = ±10.8%, 81 data points). Despite comparable accuracy, the model involving the changing reaction mechanism and TAG mass transfer limitations is recommended due to its computational simplicity and consistent applicability.

Keywords: Biodiesel, hemp seed oil, methanolysis, kinetic, quicklime

Introduction

Climate change and the increasing cost of conventional energy sources have intensified research efforts aimed at discovering and developing sustainable alternatives, among which biodiesel has gained considerable attention. Chemically, biodiesel consists of alkyl esters (most commonly methyl esters) of fatty acids and represents a renewable substitute for fossil diesel. Due to reduced levels of aromatic compounds, sulfur, and heavy metals, biodiesel contributes to the reduction of greenhouse gas emissions and environmental pollution [1].

Biodiesel is typically produced via the transesterification of triacylglycerols (TAG) derived from vegetable, animal, algal, or waste-based oils and fats using alcohols with short carbon chains, usually methanol and ethanol [2]. To enhance the efficiency of this process and reduce reaction time, various catalytic systems are employed, including acidic [3], basic [4], and enzymatic catalysts [5]. Additionally, process intensification techniques such as ultrasound [6], microwave irradiation [7], and the use of co-solvents [8] have been explored. Early biodiesel production processes primarily relied on edible oils, which presented a significant economic and ethical concern in developing countries due to competition with the food supply. Therefore, extensive research has been directed towards identifying and utilizing low-cost, non-edible, or waste oil feedstocks that are both readily available and environmentally sustainable [1]. In this context, hemp seed oil (HSO) has emerged as a valuable candidate among non-edible and sustainable feedstocks for biodiesel production, owing to its favorable chemical composition and availability [9,10].

Hemp (*Cannabis sativa* L), a dicotyledonous plant belonging to the genus *Cannabis* in the family Cannabaceae, is native to Asia [11]. All parts of the plant are utilized across a wide range of industries, including food, cosmetics, paper, textile, composite materials, and chemical manufacturing, as well as renewable energy production [12,13]. Its global cultivation in over 47 countries [14] and the incorporation of its derivatives in approximately 25,000 products [15] reflect its economic and ecological

***Author address**: Milan D. Kostić, University of NIš, Faculty of Technology, Bulevar Oslobođenja 124, 16000 Leskovac, Serbia
E-mail address: milankostic285@yahoo.com, milan@tf.ni.ac.rs
The manuscript received: June 9, 2025
Paper accepted: July 8, 2025

significance. Notably, hemp seeds contain a considerable amount of oil (25%-35%), making them a promising raw material for biodiesel production [16].

Table 1. A review of the utilization of HSO as a feedstock for biodiesel production

Catalyst	Methanol-to-oil molar ratio, mol/mol	Catalyst concentration, %	Reaction temperature, °C / pressure, MPa	Reaction time, min / agitation intensity, rpm	Maximum FAME yield, % / optimal reaction conditions	Remarks	Reference
Cu/SrO[a]	12:1	3	180 / 3	180 / 1000	96±2 / CuO loading 10%	Testing the catalytic performance of Cu/SrO for transesterification and selective hydrogenation	[24]
NaOH	6:1	1	65	180	98±1.1		
KOH	6:1	0.34-1.35	60	120 / 600	75.9 / 6:1 mol/mol, 0.67%, 60 °C, 120 min	The optimization of catalyst concentration	[19]
NaOH	6:1	0.34-1.35	60	120 / 600	74.36 / 6:1 mol/mol, 0.67%, 60 °C, 120 min		
Cu/SrO[a]	3:1-15:1	3	60-220 / 0-5	30-300 / 1000	96 / Cu/SrO loading 10%, 12:1 mol/mol, 3%, 60 °C, 180 min	Testing the catalytic performance of catalysts for transesterification and selective hydrogenation; Optimization of reaction conditions	[26]
KOH	3.5:1-8:1	0.58-1.42	23.2-56.8	up 180 / 600	98.5 / 6.4:1 mol/mol, 1.2%, 43.4 °C, 30 min[d] 97.5 / 8.5:1 mol/mol, 1%, 56.8 °C, 12 min[e]	Optimization of reaction conditions	[20]
$NaOCH_3$	3:1-9:1	0.25-1.50	45-65	30-90 / 600	86.01 / 7.5:1 mol/mol, 0.8%, 53 °C, 65 min[d]	Optimization of reaction conditions	[36]
NaOH	6:1	1	70	120 / 600	92	Testing biodiesel and its blends with diesel in diesel engines	[25]
KOH	3:1-7:1	0.5-1.25	50-65 / 0.3	20	97.5 / 6:1 mol/mol, 1%, 60 °C, 20 min	Testing a hydrodynamic cavitation reactor; Optimization of reaction conditions	[21]
KOH	4:1-8:1	0.5-1.5	60	5-100	>95 / 6:1 mol/mol, 0.9%, 60 °C, 70 min	Optimization of reaction conditions; cost and energy efficiency analysis	[9]
KOH	6:1	1	60	4 / 600	>95	Influence of the fatty acid composition of the oil on transesterification kinetics	[22]
KOH	6:1-12:1	0.6-1.2	30-60	60-120	96.87 / 12:1 mol/mol, 0.9%, 45 °C, 120 min[f]	Optimization of reaction conditions	[23]
KOH	4:1	0.5[c]	36.82	10 / 1000	98.7	The effect of a new solvent; Testing biodiesel and its blends with diesel in diesel engines	[11]
WO_3[b]	3:1-12:1	0.14-0.26	50-110	60-180 / 650	91 / 7:1 mol/mol, 0.2%, 80 °C, 120 min[d]	Testing the catalytic performance of WO_3 for transesterification; Optimization of reaction conditions	[27]
KOH	2:1-10:1	0.4-1.2	50-70	20-100 / 800	95.24 / 7.41:1 mol/mol, 0.8%, 61.92 °C, 62.83 min[d]	Optimization of reaction conditions	[10]
Quicklime	6:1-12:1	3-7	60	20-60	99.1 / 6:1 mol/mol, 6.8%, 60 °C, 45 min[d]	Optimization of reaction conditions	[28]

[a] CuO loading 1%-30%; [b] nano catalyst; [c] addition of 11.2 mL patent solvent; [d] determined by response surface methodology; [e] determined by artificial neural network model combined with a genetic algorithm; [f] Taguchi approach.

Biodiesel derived from HSO has demonstrated favorable physicochemical and combustion properties, further supporting its potential as an alternative fuel. For example, Asokan et al. [17] evaluated diesel engine performance using blends of HSO biodiesel with conventional diesel, reporting optimal performance with a 20% HSO biodiesel blend. All tested blends (20%, 30%, and 40% of HSO biodiesel) resulted in reduced CO, HC, and NOx emissions compared to pure fossil diesel. Similarly, Nagwan et al. [18] showed that a blend of fossil diesel with 20% HSO biodiesel and 10% ethanol improved thermal efficiency and reduced fuel consumption relative to conventional diesel. These results reinforce the potential of HSO biodiesel as a viable and environmentally friend-

ly alternative fuel. Most studies on biodiesel production from HSO have focused on homogeneous catalysis, while investigations involving heterogeneous catalysts remain relatively scarce (Table 1). Among homogeneous catalysts, KOH has been the most frequently employed [9-11,19-23], followed by NaOH [19, 24, 25]. In contrast, only a few studies have investigated heterogeneous catalysts for HSO methanolysis [24, 26-28], which highlights the need for further research in this area. As summarized in Table 1, while some studies have explored the catalytic performance of solid catalysts, none have addressed the kinetic modeling of heterogeneously catalyzed HSO methanolysis. To support further development in this area, the present study evaluates two kinetic models for describing the quicklime-catalyzed methanolysis of HSO. The first is a pseudo-first order kinetic model that assumes the reaction progresses through two distinct stages: an initial phase limited by TAG mass transfer, followed by a chemically controlled phase. Accordingly, the model employs two separate rate equations to reflect the change in the rate-determining step over time [29]. This model has been successfully applied to various biodiesel production processes [8, 29-32]. The second approach is a comprehensive kinetic model established by Miladinović and co-authors [33] for quicklime-catalyzed methanolysis of sunflower oil. It integrates the changing reaction mechanism and TAG mass transfer limitations and describes the reaction kinetics through the entire reaction period using a single equation. The reliability and practical utility of this model have been demonstrated in several studies [8, 30, 32, 34, 35].

In this study, a two-step process was employed to produce fatty acid methyl esters (FAMEs) from HSO. The first step involved the esterification of free fatty acids (FFAs) in the HSO catalyzed by H_2SO_4, followed by methanolysis of the esterified oil in the presence of quicklime. The main objective of this study was to evaluate the applicability and accuracy of the two kinetic models for describing the kinetics of HSO methanolysis. Model validity was assessed by comparing calculated and experimental TAG conversion degree values. Our previous study demonstrated that quicklime is an effective catalyst for HSO methanolysis, and optimal reaction conditions for maximum oil conversion were established [28]. To the best of our knowledge, this is the first kinetic study of heterogeneously catalyzed HSO methanolysis.

Materials and methods

Materials

HSO was obtained by screw pressing of hemp seeds (Versele-Laga, Belgium) purchased from a local pet shop. The pressing procedure and the physicochemical properties of the obtained HSO are described in our previous study [28]. Quicklime was acquired from a local supplier (Leskovac, Serbia), while methanol (99.5%) and Na_2SO_4 were obtained from Zorka Pharma-Hemija (Serbia). Concentrated H_2SO_4 was supplied by Lach-Ner (Czech Republic). Methanol and n-hexane (both HPLC grade) were procured from Promochem LGC (Germany), whereas 2-propanol (HPLC grade) was obtained from Carlo Erba (Italy).

FAME synthesis

FAME synthesis was carried out via a sequential two-stage method, comprising the esterification of FFA under acidic conditions, followed by the alkali-catalyzed methanolysis of the resulting esterified HSO. This approach was necessary due to the high acid value (2.98 mg KOH/g) of the obtained HSO [28], which exceeds the threshold of 1 mg KOH/g, commonly considered as the upper limit for direct alkali-catalyzed transesterification.

FFA esterification

FFA esterification was conducted using methanol and H_2SO_4 as a catalyst under the following reaction conditions: a catalyst amount of 2% of HSO mass, a methanol-to-HSO molar ratio of 8.5:1, and a reaction temperature of 45 °C. These conditions were selected based on the optimization study reported by Kostić et al. [37]. The acid value of HSO was reduced to 0.58 mg KOH/g oil [28] through the esterification process, enabling its subsequent application in biodiesel production via quicklime-catalyzed methanolysis.

Methanolysis of the esterified HSO

Quicklime-catalyzed methanolysis was conducted under varying reaction conditions, including catalyst amounts of 3%, 5%, and 7% of the esterified HSO mass, methanol-to-HSO molar ratios of 6:1, 9:1, and 12:1, and a temperature of 60 °C. Prior to use, the quicklime was ground, and the fraction with a particle size of 0.5 mm was further calcined at 550 °C for 4 h. The characteristics of the calcined quicklime have been described elsewhere [33]. The methanolysis reaction was performed following the procedure described by Kostić et al. [37]. The qualitative and quantitative composition of the ester-oil phase was determined using high-performance liquid chromatography (HPLC) [38].

Kinetics of the esterified HSO methanolysis

The kinetics of the methanolysis reaction was evaluated using two different kinetic models: pseudo-first order kinetic model and the model involving a changing reaction mechanism coupled with TAG mass transfer limitations (Table 2). The heterogeneously catalyzed methanolysis reaction proceeds through two distinct regimes: an initial heterogeneous regime, where the reaction rate is controlled by TAG mass transfer resistance, followed by a pseudo-homogeneous regime, where the chemical reaction limits the reaction rate [29,30]. The reaction kinetics in both regimes were analyzed using a pseudo-first order model (Eqs. 1 and 3, Table 2). The second model (Eq. 5, Table 2), which involves changes in the reaction mechanism and TAG mass transfer limitation, describes the kinetics of the methanolysis across the entire reaction period [30, 33].

Table 2. Kinetic models for the HSO methanolysis

Kinetic model[a]		Equation	Eq. number
Pseudo-first order kinetic model	Heterogeneous regime	$-\ln(1-x_A) = k_c a \cdot t$	1
		$x_A = 1-\exp(-k_c a \cdot t)$	2
	Pseudo-homogeneous regime	$-\ln(1-x_A) = k_{app} \cdot t + C_1$	3
		$x_A = 1-\exp(-k_{app} \cdot t - C_1)$	4
Model involving the changing reaction mechanism and TAG mass transfer limitation		$\frac{dx_A}{dt} = \frac{3k_m(1-x_A)\cdot\left(\frac{c_{R0}}{3c_{A0}}+x_A\right)}{\frac{K}{c_{A0}}+1-x_A}$	5
Simplified form (if $3c_{A0} \gg c_{R0}$)		$\frac{dx_A}{dt} = \frac{3k_m(1-x_A)x_A}{\frac{K}{c_{A0}}+1-x_A}$	6

[a] x_A – the TAG conversion degree (1); $k_c a$ – the volumetric TAG mass transfer coefficient (min^{-1}); k_{app} – the apparent pseudo-first order reaction rate constant (min^{-1}); k_m – the apparent reaction rate constant for the model involving the changing reaction mechanism and TAG mass transfer limitation; K – the parameter defining the affinity of TAG to the active sites of the catalyst; c_{A0} – the initial TAG concentration (mol/dm^3); c_{R0} – the hypothetical initial FAME concentration corresponding to the initial available active catalyst (mol/dm^3); t – time (min); C_1 – the integration constant.

The accuracy of the models was assessed using the mean relative percent deviation (*MRPD*) calculated according to Eq. 7:

$$\mathrm{MRPD} = \frac{100}{n}\sum_{i=1}^{n}\left|\frac{y_{p,i}-y_{a,i}}{y_{a,i}}\right| \quad (7)$$

where y_p and y_a are predicted and experimental values of the TAG conversion degree (%), respectively, and n is the number of experimental runs.

Results and discussion

Methanolysis reaction analysis

Changes in the composition of the reaction system over time during the methanolysis of the esterified HSO catalyzed by quicklime are shown in Fig. 1. The increase in FAME content exhibited a sigmoidal trend, indicating that the methanolysis of HSO progressed through three periods. In the initial reaction period, FAME formation was slow, followed by a period of fast reaction, after which the reaction rate gradually declined as the reaction approached completion. As the FAME content increased, the TAG content decreased accordingly. The content of intermediate products, monoacylglycerols (MAGs) and diacylglycerols (DAGs), initially increased, reaching a maximum at intermediate time points, then declined and finally remained nearly constant. Notably, the content of MAGs and DAGs did not exceed 4% and 1%, respectively, for the entire reaction time. The observed kinetic behavior is typical of heterogeneously catalyzed methanolysis reactions [29, 31, 33]. The low reaction rate in the initial reaction period is attributed to TAG mass transfer limitations arising from the immiscibility of methanol and oil, as the catalyst is initially saturated with methanol. As the reaction progressed, the formation of FAME improved the miscibility of the reactants by acting as a co-solvent, thereby facilitating the adsorption of TAG onto the active sites of the catalyst, where the methanolysis reaction occurs [29].

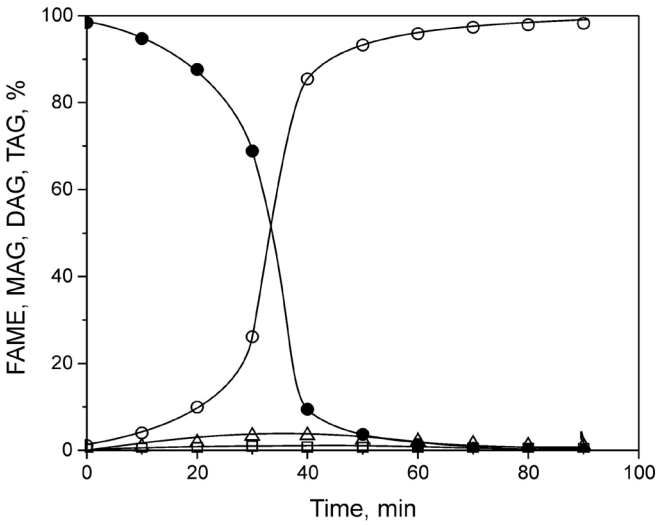

Figure 1. Variation in reaction mixture composition over time during quicklime-catalyzed methanolysis of esterified HSO (reaction conditions: 60 °C; methanol-to-HSO molar ratio 6:1, catalyst amount 3%; TAG - •; FAME - ○; MAG - Δ; DAG – □)

Kinetics of esterified HSO methanolysis

The kinetic parameters of the pseudo-first order model, $k_c a$ and k_{app}, were determined using Eqs. 1 and 3 (Table 2), respectively. These equations describe the kinetics of the reaction in two distinct regimes of the reaction: the initial regime, controlled by TAG mass transfer resistance, and the later regime, limited by the chemical reaction. The experimental data for x_A were first fitted using the sigmoidal Boltzmann function, after which the values of $-\ln(1-x_A)$ were calculated. The dependences of $-\ln(1-x_A)$ on reaction time are shown in Fig. 2, while the kinetic parameters $k_c a$ and k_{app}, obtained as the slopes of the corresponding linear dependences, are presented in Table 3. The model's performance, indicated by high R^2 values, demonstrated its validity in describing the experimental data.

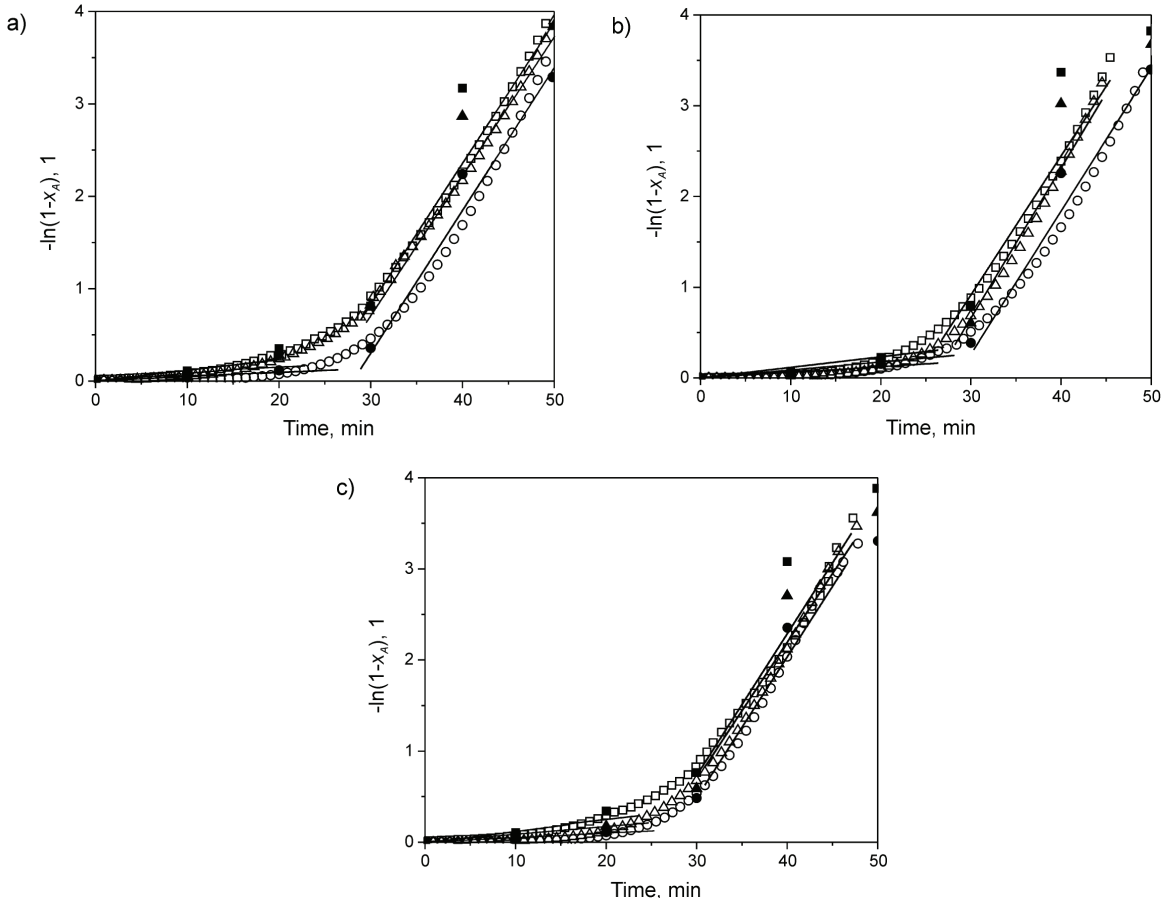

Figure 2. Dependence $-\ln(1-x_A)$ vs. t during quicklime-catalyzed methanolysis of esterified HSO at methanol-to-HSO molar ratio 6:1 (a), 9:1 (b), and 12:1 (c) (reaction temperature: 60 °C; catalyst amount: 3% – ●, 5% – ▲, 7% – ■; experimental data – solid symbols; sigmoidally fitted values – open symbols)

Table 3. Parameter values of the applied kinetic models[a]

Methanol-to-HSO molar ratio, mol/mol	Catalyst amount, % of HSO mass	$k_c a$, min^{-1}	R^2	k_{app}, min^{-1}	R^2	k_m, min^{-1}	K, mol/dm^3	R^2
6:1	3	0.0048	0.965	0.154	0.979	0.156	1.081	0.932
	5	0.0082	0.915	0.153	0.992	0.155	1.404	0.975
	7	0.0116	0.949	0.151	0.987	0.156	1.808	0.987
9:1	3	0.0062	0.898	0.158	0.977	0.152	1.168	0.926
	5	0.0088	0.929	0.165	0.985	0.159	1.284	0.923
	7	0.0116	0.916	0.153	0.982	0.159	1.763	0.980
12:1	3	0.0050	0.924	0.155	0.971	0.159	1.022	0.974
	5	0.0056	0.907	0.155	0.982	0.155	1.211	0.967
	7	0.0128	0.926	0.151	0.986	0.150	1.081	0.979
				0.155±0.004		0.155±0.003		

[a] $k_c a$ – the volumetric TAG mass transfer coefficient; k_{app} – the apparent pseudo-first order reaction rate constant; k_m – the apparent reaction rate constant for the model involving the changing reaction mechanism and TAG mass transfer limitation; K – the constant defining the affinity of TAG to the active sites of the catalyst; R^2 – coefficient of determination.

The parameters of the kinetic model involving a changing reaction mechanism coupled with TAG mass transfer limitation (k_m, K, and c_{R0}; Eq. 5, Table 2) were calculated through nonlinear regression fitting using the Levenberg-Marquardt algorithm in Polymath. Under the applied reaction conditions, the values of $3c_{A0}$, which ranged from 2.01 to 2.42 mol/dm^3, were significantly higher than the determined c_{R0} values (up to 0.006 mol/dm^3). Therefore, the simplified form of the proposed kinetic model (Eq. 6, Table 2) was used to model the kinetics of quicklime-catalyzed HSO methanolysis [30]. The determined values of the apparent reaction rate constant (k_m) and the constant defining the affinity of TAG to the active sites of the catalyst (K) of this kinetic model (Eq. 6, Table 2) are presented in Table 3. The high R^2 values validated the model's capability to describe the kinetics of esterified HSO methanolysis catalyzed by quicklime. The values of parameter K were only slightly higher than the initial TAG concentrations (c_{A0} in the range 0.67 - 0.81 mol/dm^3) and thus, the kinetic model was not further simplified [34].

Effect of the reaction conditions on kinetic parameters

The influence of catalyst concentration and methanol-to-HSO ratio on the kinetic parameters of both kinetic models is presented in Fig. 3. The volumetric TAG mass transfer coefficient k_ca of the pseudo-first order kinetic model and the parameter K, which defines the affinity of TAG to the catalyst's active sites in the model involving a changing reaction mechanism coupled with TAG mass transfer limitations, were independent of the methanol concentration but increased proportionally with the catalyst concentration (Fig. 3a and c).

The influence of reaction conditions on the kinetic parameters k_ca and K was statistically evaluated through analysis of variance (ANOVA) using a linear regression model (Table 4). According to the ANOVA results, the model was statistically significant (p=0.0031), which was further confirmed based on the values of the coefficient of determination (R^2), adjusted (R^2_{adj}), and predicted (R^2_{pred}) coefficients of determination (Table 4) as well as on internal model selection criteria in Design Expert software. F- and p- values indicated that catalyst concentration had a statistically significant effect on both kinetic parameters, whereas the effect of initial methanol concentration was not statistically significant. Consequently, k_ca and K were correlated with the catalyst concentration, as described by Eqs. 8 and 9 (R^2 = 0.981 and R^2 = 0.982, respectively):

$$k_ca=0.014\cdot c_{cat} \quad (8)$$

$$K=2.334\cdot c_{cat} \quad (9)$$

where c_{cat} is catalyst concentration (mol/dm^3).

A similar effect of catalyst concentration on volumetric TAG mass transfer coefficient, k_ca, has been observed for methanolysis of sunflower oil catalyzed by CaO [29]. However, in the methanolysis of sour cherry kernel oil over CaO, neither catalyst concentration nor methanol amount influenced k_ca [31]. A linear increase in k_ca with the initial methanol and catalyst concentrations was observed in the case of *Sinapis alba* seed oil methanolysis catalyzed by quicklime [30].

On the other hand, previous studies have reported that parameter K increases with increasing catalyst concentration and methanol amount in quicklime-catalyzed methanolysis of sunflower oil [33] and *S. alba* seed oil [30]. Since K represents the affinity of TAG for the catalyst active sites, its increase with increasing the catalyst concentration can be attributed to the greater availability of catalytically active sites [33]. The influence of methanol concentration on parameter K depends on the range of initial methanol-to-oil molar ratio [33] and the fatty acid composition of the used oil [30].

Table 4. ANOVA results of the effect of reaction conditions on k_ca and K

Parameter		Sum of squares	df	Mean square	F–value	p–value
k_ca[a]	Model	6.5·10^{-5}	2	3.3·10^{-5}	17.58	**0.0031**[c]
	Initial methanol concentration	2.0 ·10^{-6}	1	2.0·10^{-6}	1.08	0.3384
	Catalyst concentration	6.5·10^{-5}	1	6.5·10^{-5}	35.06	**0.0010**[c]
	Residual	1.1·10^{-5}	6	1.9·10^{-6}		
	Cor Total	7.6·10^{-5}	8			
K[b]	Model	0.739	2	0.370	33.11	**0.0006**[c]
	Initial methanol concentration	0.009	1	0.009	0.778	0.4118
	Catalyst concentration	0.728	1	0.7289	65.24	**0.0002**[c]
	Residual	0.067	6	0.011		
	Cor Total	0.806	8			

[a] R^2=0.854; R^2_{adj}=0.806; R^2_{pred}=0.688; *Adeq. Precision*=9.15; [b] R^2=0.917; R^2_{adj}=0.889; R^2_{pred}=0.830; *Adeq. Precision*=12.82;
[c] Statistically significant at the 95% confidence level.

The apparent reaction rate constants for both kinetic models, k_{app} and k_m, remained nearly constant under all investigated reaction conditions, indicating their independence from both the catalyst concentration and initial methanol concentration (Fig. 3b and d). Therefore, their mean values were calculated. It should be noted that the mean values of k_{app} and k_m were identical for both kinetic models (k_{app} = 0.155±0.004 min^{-1} and k_m = 0.155±0.003 min^{-1}).

The independence of k_{app} from the catalyst concentration and methanol amount has also been reported for CaO-catalyzed methanolysis of sour cherry kernel oil [31], *S. alba* seed oil [30], and sunflower oil [29]. The k_{app} value obtained for HSO methanolysis in this study (0.155±0.004 min^{-1}) is higher than that reported for the methanolysis of sunflower oil (0.07 min^{-1}) [29], *S. alba* oil (0.114 min^{-1}) [30], and sour cherry kernel oil (0.084 min^{-1}) [31], but lower compared to palm oil methanolysis (0.2898 min^{-1}) [39], all catalyzed by CaO and conducted at the same reaction temperature (60 °C). Observed differences in reaction rate constants, despite the use of the same catalytic system, are predominantly attributed to the type of oily feedstock. In particular, the degree of unsaturation and the fatty acid chain length have been reported as key factors influencing the kinetics of the methanolysis reaction [40, 41]. Additionally, the reaction rate constant of the pseudo-first order kinetic model was linearly correlated with the unsaturation degree of the oily feedstock [22]. Previous studies that applied a kinetic model involving a changing reaction mechanism and TAG mass transfer limitation to describe the kinetics of sunflower oil [33] and *S. alba* oil [30] methanolysis reported that the apparent reaction rate constant k_m depends on the catalyst and initial methanol concentrations. However, no in-depth analysis of this dependency was conducted.

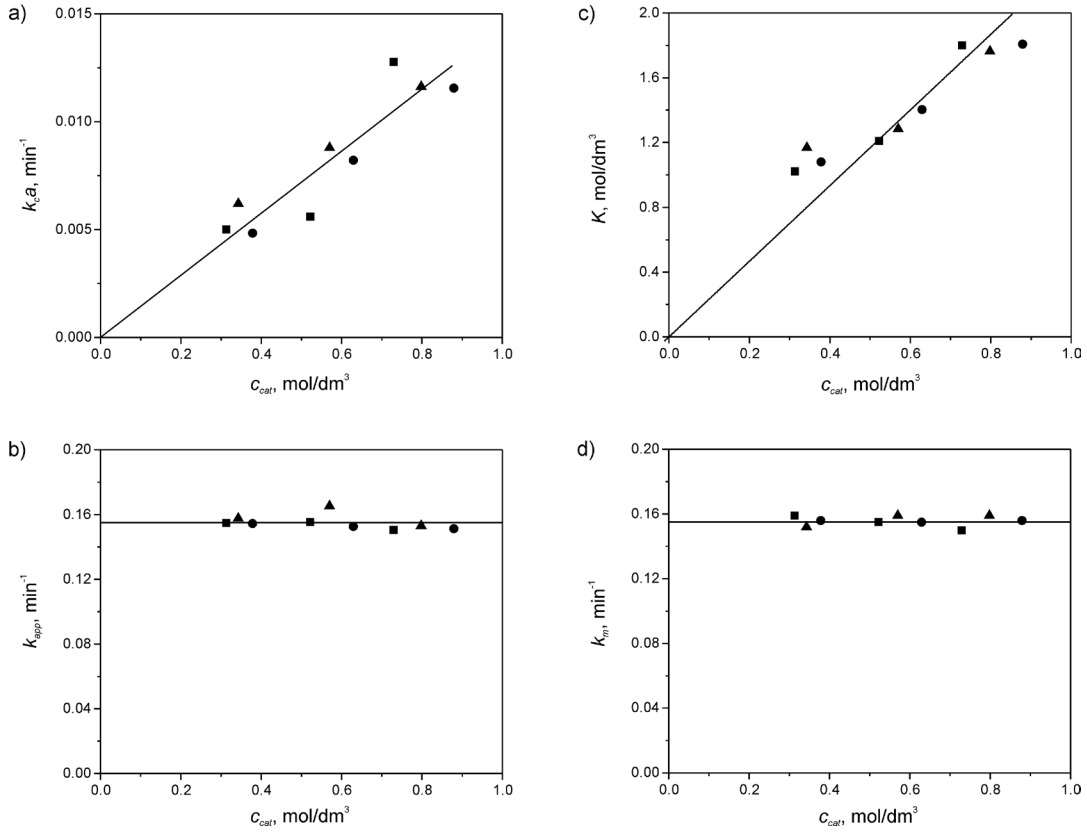

Figure 3. Dependence of kinetic model parameters $k_c a$ (a), k_{app} (b), K (c), and k_m (d) on the catalyst concentration at different methanol-to-HSO molar ratios: 6:1 – •; 9:1 – ▲; 12:1 – ■

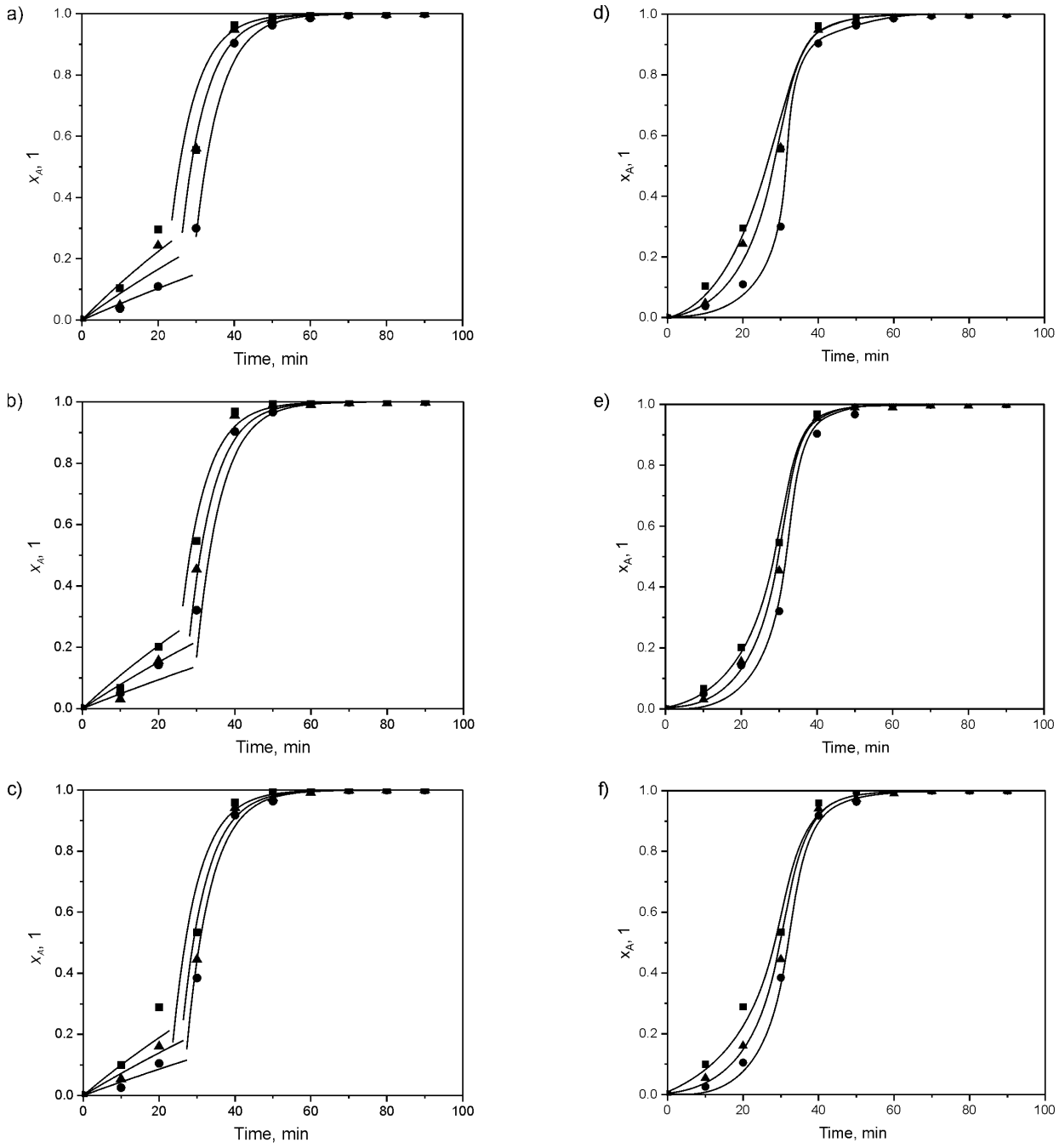

Figure 4. Comparison of experimental (symbols) and calculated (lines) TAG conversion degree values based on the pseudo-first order kinetic model (a-c) and the model involving changing reaction mechanism and TAG mass transfer limitations (d-f) for quicklime-catalyzed HSO methanolysis at methanol-to-HSO molar ratios of 6:1 (a, d), 9:1 (b, e) and 12:1 (c, f) (reaction temperature: 60 °C; catalyst amount: 3% – ●, 5% – ▲, and 7% – ■)

Simulation of methanolysis of the esterified HSO

The accuracy of the applied kinetic models in simulating the methanolysis of esterified HSO was evaluated by comparing experimental and model-predicted values of TAG conversion degree. For the pseudo-first order kinetic model, x_A was calculated using Eqs. 2 and 8 in the heterogeneous reaction regime, and Eq. 4 and the mean value of k_{app} in the pseudo-homogeneous regime. For the kinetic model that incorporates a changing reaction mechanism and mass transfer limitations of TAG, x_A was calculated using Eqs. 6 and 9, and the mean value of k_m, using Polymath software.

As shown in Fig.4 a-c, a good agreement was observed between the experimental x_A values and values calculated based on the pseudo-first order kinetic model. This is further confirmed by the low mean relative percentage deviation (*MRPD*) of ±10.8% (based on 81 data points). Therefore, the proposed kinetic model is

suitable for describing the kinetics of HSO methanolysis catalyzed by quicklime. The same model has been successfully applied to describe the kinetics of methanolysis of sunflower oil [29, 32, 35, 42], *S. alba* oil [30], used vegetable oil [42], and sour cherry kernel oil [31], all catalyzed by CaO-based catalysts.

The applicability of the model involving a changing reaction mechanism coupled with TAG mass transfer limitations was also proven by comparing the experimental and calculated TAG conversion degree values. As can be visually concluded from Fig. 4d-f, the experimental x_A values closely match those predicted by the kinetic model, which is also supported by the low *MRPD* value (±10.1%, based on 81 data points). The obtained results indicated the reliability of the model involving changing reaction mechanism and TAG mass transfer limitation in describing the kinetics of the esterified HSO methanolysis reaction over quicklime. The validity of this model has also been established for the methanolysis of white mustard seed oil [30]. The simplified form of the model involving a changing reaction mechanism and TAG mass transfer limitation was successfully applied in describing the kinetics of CaO-based catalyzed methanolysis of various oily feedstocks: black mustard seed oil [8], sour cherry kernel oil [31], rapeseed oil [34], and sunflower oil [32, 35, 43]. Considering its demonstrated suitability for CaO-catalytic systems, the applied kinetic model shows strong potential for broader application to other feedstocks and solid catalysts, and its further validation is recommended through extended studies.

Conclusion

This study demonstrated that the kinetics of quicklime-catalyzed methanolysis of esterified HSO can be accurately described using two kinetic models: a pseudo-first order model and a model involving a changing reaction mechanism coupled with TAG mass transfer limitations. The pseudo-first order model successfully described the reaction kinetics across two regimes: an initial mass transfer-limited regime and a subsequent chemically controlled regime. In contrast, the second model provided a unified approach, effectively representing the reaction kinetics throughout the entire reaction period. ANOVA analysis revealed that the kinetic parameters $k_c a$ and K were independent of methanol concentration but increased with the catalyst concentration. The apparent reaction rate constant was unaffected by the applied reaction conditions and had the same value (0.155 min^{-1}) for both models. The reliability of the models was demonstrated by good agreement between experimental and predicted TAG conversion degree values, as indicated by low *MRPD* values (±10.8% and ±10.1% across 81 data points). Although both models proved reliable, the model involving the changing reaction mechanism and TAG mass transfer limitation is recommended due to its computational simplicity and ability to describe the entire reaction course without regime segmentation. Overall, these findings offer valuable insights into the kinetics of heterogeneously catalyzed biodiesel production and support further development of solid catalyst systems for sustainable biodiesel production.

Nomenclature

Abbreviations	
TAG	Triacylglycerols
HSO	Hemp seed oil
FFA	Free fatty acid
FAME	Fatty acid methyl esters
HPLC	High-performance liquid chromatography
MRPD	Mean relative percentage deviation
Symbols	
x_A	TAG conversion degree (1)
$k_c a$	Volumetric TAG mass transfer coefficient (min^{-1})
t	Reaction time (min)
k_{app}	Apparent pseudo-first order reaction rate constant (min^{-1})
C_1	Integration constant (1)
k_m	Apparent reaction rate constant for the model involving the changing reaction mechanism and TAG mass transfer limitation (min^{-1})
K	Constant defining the affinity of TAG to the active sites of the catalyst (mol/dm^3)
R^2	Coefficient of determination (1)
c_{A0}	Initial TAG concentration (mol/dm^3)
c_{B0}	Initial concentration of methanol (mol/dm^3)
c_{cat}	Concentration of catalyst (mol/dm^3)
c_{R0}	Hypothetical initial FAME concentration (mol/dm^3)

Acknowledgments

This work was supported by the Republic of Serbia - Ministry of Science, Technological Development and Innovation of Serbia, Programs for Financing Scientific Research Work, No. 451-03-137/2025-03/ 200133 (Project assigned to the Faculty of Technology, Leskovac, University of Niš)

References

[1] Malabadi RB, Kolkar KP, Chalannavar RK. Industrial *Cannabis sativa*: Hemp oil for biodiesel production. *Magna Scientia Advanced Research and Reviews.* 2023, 09, 022-035. https://doi.org/10.30574/msarr.2023.9.2.0145

[2] Avhad MR, Marchetti JM. A review on recent advancement in catalytic materials for biodiesel production. *Renewable and Sustainable Energy Reviews*. 2015, 50, 696-718. https://doi.org/10.1016/j.rser.2015.05.038

[3] Aliyu M, Moser BR, Alharthi FA, Rashid U. Efficient production of biodiesel from palm fatty acid distillate using a novel hydrochar-based solid acid catalyst derived from palm leaf waste. *Process Safety and Environmental Protection*. 2024, 187, 1126-1139. https://doi.org/10.1016/j.psep.2024.05.040

[4] Ribeiro TS, Sobrinho IA, Gonçalves MA, Lima VS, Figueira BAM, Filho GNR, da Conceição LRV. Green synthesis of biodiesel from magnetic basic biochar derived from *Amazonian murici* residual biomass: Optimization, kinetic, thermodynamic, and environmental studies. *Journal of Environmental Chemical Engineering*. 2024, 12, 114725. https://doi.org/10.1016/j.jece.2024.114725

[5] Pasha MK, Rahim M, Dai L, Liu D, Du W, Guo M. Comparative study of a two-step enzymatic process and conventional chemical methods for biodiesel production: Economic and environmental perspectives. *Chemical Engineering Journal.* 2024, 489, 151254. https://doi.org/10.1016/j.cej.2024.151254

[6] Rehab MA, Eslam S, Hesham AH. A novel technology for microwave-assisted synthesis of new Ca/Si/Al composite

oxide-based catalyst for boosting the ultrasound-assisted biodiesel production. *Process Safety and Environmental Protection.* 2025, 194, 674-687. https://doi.org/10.1016/j.psep.2024.12.042

[7] Oladipo B, Qasana S, Zini SC, Menemene N, Ojumu TV. Microwave-assisted biodiesel synthesis from waste cooking oil: Exploring the potential of carob pod-derived solid base catalyst. *Fuel Processing Technology.* 2024, 266, 108161. https://doi.org/10.1016/j.fuproc.2024.108161

[8] Đorđević BS, Kostić MD, Todorović ZB, Stamenković OS, Veselinović LjM, Veljković VB. Triethanolamine-based deep eutectic solvents as cosolvents in biodiesel production from black mustard (*Brassica nigra* L.) seed oil. *Chemical Engineering Research and Design.* 2023, 195, 526-536. https://doi.org/10.1016/j.cherd.2023.06.016

[9] Samuel OD, Boye TE, Enweremadu CC. Financial and parametric study of biodiesel production from hemp and tobacco seed oils in modified fruit blender and prediction models of their fuel properties with diesel fuel. *Bioresource Technology Reports.* 2020, 12, 100599. https://doi.org/10.1016/j.biteb.2020.100599

[10] Yazilitas C, Zeki Yilbas Z, Yesilyurt MK. Biodiesel production from hempseed (*Cannabis sativa* L.) oil: Providing optimum conditions by response surface methodology. *Science and Technology for Energy Transition*. 2024, 79, 11, https://doi.org/10.2516/stet/2024006

[11] Bhonsle AK, Rawat N, Trivedi J, Singh R, Singh J, Atray N. Biodiesel production using novel solvent from agricultural crop *Cannabis sativa* L. and *Sapium sebiferum* L. and their fuel properties characterisation using blends. *Bioresource Technology Reports.* 2023, 23, 101555. https://doi.org/10.1016/j.biteb.2023.101555

[12] Aryal K, Maraseni T, Kretzschmar T, Chang D, Naebe M, Neary L, Ash G. Knowledge mapping for a secure and sustainable hemp industry: A systematic literature review. *Case Studies in Chemical and Environmental Engineering.* 2024, 9, 100550. https://doi.org/10.1016/j.cscee.2023.100550

[13] Wirtshafter DE. Ten years of a modern hemp industry. *Journal of Industrial Hemp.* 2024, 9, 9-14. https://doi.org/10.1300/J237v09n01_03

[14] Burton R, Andres M, Cole M, Cowley J, Augustin M. Industrial hemp seed: from the field to value-added food ingredients. *Journal of Cannabis Research.* 2022, 4. https://doi.org/10.1186/s42238-022-00156-7

[15] Sebastian J, Dong X, Trostle C, Pham C, Joshi M, Jessup R, Burow M, Provin T. Hemp Agronomy: Current Advances, Questions, Challenges, and Opportunities. *Agronomy*. 2023, 13, 475. https://doi.org/10.3390/agronomy13020475

[16] Leizer C, Ribnicky D, Poulev A, Dushenkov S, Raskin I. The composition of Hemp seed oil and its potential as an important source of nutrition. *Journal of Nutraceuticals, Functional & Medical Foods*. 2000, 2, 3553. https://doi.org/10.1300/J133v02n04_04

[17] Asokan MA, Senthur Prabu S, Bollu A, Abhinay Reddy M, Ram A, Sukhadia DS. Emission and performance behavior of hemp seed oil biodiesel/diesel blends in DI diesel engine. *Materials Today: Proceedings*. 2021, 46, 8127-8132. https://doi.org/10.1016/j.matpr.2021.03.064

[18] Nagwan H, Bangari RS, Singh K, Kumar P. Study the performance characteristics of CI engine with hemp oil methyl Ester, ethanol and diesel blends. *Materials Today: Proceedings*. 2023. https://doi.org/10.1016/j.matpr.2023.05.108

[19] Ahmad M, Ullah K, Khan MA, Zafar M, Tariq M, Ali S, Sultana S. Physicochemical analysis of hemp oil biodiesel: A promising non edible new source for bioenergy. *Energy Sources, Part A*. 2011, 33, 1365-1374. https://doi.org/10.1080/15567036.2010.499420

[20] Stamenković OS, Veličković AV, Kostić MD, Joković NM, Rajković KM, Milić PS, Veljković VB. Optimization of KOH-catalyzed methanolysis of hempseed oil. *Energy Conversion and Management.* 2015, 103, 235-243. https://doi.org/10.1016/j.enconman.2015.06.054

[21] Khan IA, Prasad N, Pal A, Yadav AK. Efficient production of biodiesel from *Cannabis sativa* oil using intensified transesterification (hydrodynamic cavitation) method. *Energy Sources, Part A: Recovery, Utilization, and Environmental Effects.* 2019, 42, 2461-2470. https://doi.org/10.1080/15567036.2019.1607946

[22] Kostić MD, Stamenković OS, Veljković VB. The influence of fatty acid composition on the kinetics of the vegetable oil methanolysis reaction. *Advanced Technologies.* 2021, 10, 24-31. https://doi.org/10.5937/savteh2102024K

[23] Yilbaşi Z, Yesilyurt M, Arslan M. The production of methyl ester from industrial grade hemp (*Cannabis sativa* L.) seed oil: a perspective of Turkey — the optimization study using the Taguchi method. *Biomass Conversion and Biorefinery.* 2021, 13, 9955-9975. https://doi.org/10.1007/s13399-021-01751-z

[24] Yang R, Su M, Li M, Zhang J, Hao X, Zhang H. One-pot process combining transesterification and selective hydrogenation for biodiesel production from starting material of high degree of unsaturation. *Bioresource Technology*. 2010, 101, 5903-5909. https://doi.org/10.1016/j.biortech.2010.02.095

[25] Afif MK, Biradar CH. Production of biodiesel from *Cannabis sativa* (Hemp) seed oil and its performance and emission characteristics on DI engine fueled with biodiesel blends. *International Journal of Engineering & Technology.* 2019, 6, 246-253. ISSN: 2395-0056

[26] Su M, Yang R, Li M. Biodiesel production from hempseed oil using alkaline earth metal oxides supporting copper oxide as bi-functional catalysts for transesterification and selective hydrogenation. *Fuel.* 2013, 103, 398-407. https://doi.org/10.1016/j.fuel.2012.07.009

[27] Abbasi TU, Ahmad M, Asma M, Rozina, Munir M, Zafar M, Katubi KM, Alsaiari NS, Yahya AEM, Mubashir M, Chuah LF, Bokhari A. High efficient conversion of *Cannabis sativa* L. biomass into bioenergy by using green tungsten oxide nano-catalyst towards carbon neutrality. *Fuel.* 2023, 336, 126796. https://doi.org/10.1016/j.fuel.2022.126796

[28] Đorđević BS, Kostić MD, Miladinović MR, Stamenković OS. Optimization of quicklime-catalyzed biodiesel production from hemp (*Cannabis sativa* l.) seed oil. *Advanced Technologies.* 2025, 14(1), 35-45. https://doi.org/10.5937/savteh2501034D

[29] Veljković VB, Stamenković OS, Todorović ZB, Lazić ML, Skala DU. Kinetics of sunflower oil methanolysis catalyzed by calcium oxide. *Fuel*. 2009, 88, 1554-1562. https://doi.org/10.1016/j.fuel.2009.02.013

[30] Kostić MD, Djalović IG, Stamenković OS, Mitrović PM, Adamović DS, Kulina MK, Veljković VB. Kinetic modeling and optimization of biodiesel production from white mustard (*Sinapis alba* L.) seed oil by quicklime–catalyzed transesterification. *Fuel.* 2018, 223, 125-139. https://doi.org/10.1016/j.fuel.2018.03.023

[31] Kostić MD, Đorđević BS, Miladinović MR, Stamenković OS. Biodiesel production from sour cherry kernel oil: Kinetics, thermodynamics, and optimization. *Energy Conversion and Management.* 2024, 317, 118858. https://doi.org/10.1016/j.enconman.2024.118858
[32] Pavlović SM, Marinković DM, Kostić MD, Janković-Častvan IM, Mojović LV, Stanković MV, et al. A CaO/zeolite-based catalyst obtained from waste chicken eggshell and coal fly ash for biodiesel production. *Fuel*. 2020, 267, 117171. https://doi.org/10.1016/j.fuel.2020.117171
[33] Miladinović MR, Krstić JB, Tasić MB, Stamenković OS, Veljković VB. A kinetic study of quicklime-catalyzed sunflower oil methanolysis. *Chemical Engineering Research and Design.* 2014, 92, 1740-1752. https://doi.org/10.1016/j.cherd.2013.11.023
[34] Nježić ZB, Kostić MD, Marić BD, Stamenković OS, Šimurina OD, Krstić J, Veljković V.B. Kinetics and optimization of biodiesel production from rapeseed oil over calcined waste filter cake from sugar beet processing plant. *Fuel.* 2023, 334, 126581. https://doi.org/10.1016/j.fuel.2022.126581
[35] Pavlović SM, Marinković DM, Kostić MD, Lončarević DR, Mojović LjV, Stanković MV, Veljković VB. The chicken eggshell calcium oxide ultrasonically dispersed over lignite coal fly ash-based cancrinite zeolite support as a catalyst for biodiesel production. *Fuel.* 2021, 289, 119912. https://doi.org/10.1016/j.fuel.2020.119912
[36] Rashid USG, Bhatti SG, Ansari TM, Yunus R, Ibrahim M. Biodiesel production from *Cannabis sativa* oil from Pakistan. *Energy Sources, Part A: Recovery, Utilization, Environmental Effects.* 2016, 8, 865-875. http://dx.doi.org/10.1080/15567036.2013.803179
[37] Kostić MD, Veličković AV, Joković NM, Stamenković OS, Veljković VB. Optimization and kinetic modelling of esterification of the oil obtained from waste plum stones as a pretreatment step in biodiesel production. *Waste Management.* 2016, 48, 619-629. https://doi.org/10.1016/j.wasman.2015.11.052
[38] Stamenković OS, Lazić ML, Todorović ZB, Veljković VB, Skala DU. The effect of agitation intensity on alkali-catalyzed methanolysis of sunflower oil. *Bioresource Technology*. 2007, 98, 2688–2699. https://doi.org/10.1016/j.biortech.2006.09.024
[39] Maneerung T, Kawi S, Wang C-H. Biomass gasification bottom ash as a source of CaO catalyst for biodiesel production via transesterification of palm oil. *Energy Conversion and Managemen*t. 2015, 92, 234-243. https://doi.org/10.1016/j.enconman.2014.12.057
[40] Yan S, Lu H, Liang B. Supported CaO catalysts used in the transesterification of rapeseed oil for the purpose of biodiesel production. *Energy Fuel.* 2008, 22, 646-51. https://doi.org/10.1021/ef070105o
[41] Pinzi S, Gandía LM, Arzamendi G, Ruiz JJ, Dorado MP. Influence of vegetable oils fatty acid composition on reaction temperature and glycerides conversion to biodiesel during transesterification. *Bioresource Technology* 2011, 102, 1044-50. https://doi.org/10.1016/j.biortech.2010.08.029
[42] Lukić I, Kesić Ž, Maksimović S, Zdujić M, Liu H, Krstić J, Skala D. Kinetics of sunflower and used vegetable oil methanolysis catalyzed by CaO·ZnO. *Fuel.* 2013, 113, 367-378. https://doi.org/10.1016/j.fuel.2013.05.093
[43] Kostić M, Bazargan A, Stamenković O, Veljković V, McKay G. Optimization and kinetics of sunflower oil methanolysis catalyzed by calcium oxide–based catalyst derived from palm kernel shell biochar. *Fuel.* 2016, 163, 304-313. http://dx.doi.org/10.1016/j.fuel.2015.09.042

Izvod

KINETIČKA ANALIZA I MODELOVANJE METANOLIZE ULJA SEMENA KONOPLJE KATALIZOVANE NEGAŠENIM KREČOM

Milan D. Kostić, Biljana S. Đorđević, Milica Z. Petković, Marija R. Miladinović, Olivera S. Stamenković

Tehnološki fakultet u Leskovcu, Univerzitet u Nišu, Leskovac, Srbija

(ORIGINALNI NAUČNI RAD)
UDK: 662.756.3:677.12
DOI: 10.5937/savteh2502059K

Industrijska konoplja (*Cannabis sativa* L.) je višestruko korisna biljka sa širokom primenom u različitim granama industrije, a ulje iz semena predstavlja perspektivnu sirovinu za proizvodnju biodizela. U ovom radu ispitivana je kinetika metanolize ulja iz semena konoplje (USK) katalizovane negašenim krečom. Zbog umereno povišenog sadržaja slobodnih masnih kiselina u ulju, USK je prethodno esterifikovano. Metanoliza esterifikovanog USK izvedena je pri molskim odnosima metanol:USK od 6:1, 9:1 i 12:1, količini katalizatora 3%, 5% i 7% (u odnosu na masu USK), na temperaturi 60 °C i pod atmosferskim pritiskom. Za opisivanje kinetike reakcije metanolize primenjena su dva kinetička modela: pseudo-prvi red reakcije, i model koji uključuje promenljivi mehanizam reakcije i ograničenja prenosa mase triacilglicerola (TAG). Kinetičkim modelom reakcije pseudo-prvog reda je opisana kinetika reakcije u dva jasno odvojena perioda reakcije – početni period u kome je brzina procesa kontrolisana prenosom mase TAG, koji je praćen periodom u kome hemijska reakcija određuje brzinu procesa. Nasuprot tome, drugim kinetičkim modelom kontinualno je opisana kinetika reakcije tokom celokupnog vremena njenog trajanja. Zapreminski koeficijent prenosa mase TAG ($k_c a$) i parametar koji definiše afinitet TAG ka aktivnim mestima na katalizatoru (K) povećavali su se sa povećanjem koncentracije katalizatora, ali nisu zavisili od koncentracije metanola. Prividna konstanta brzine reakcije za oba kinetička modela imala je istu vrednost (0,155 min^{-1}). Primenjeni kinetički modeli vrlo dobro opisuju kinetiku reakcije metanolize USK, što je potvrđeno dobrim slaganjem sa eksperimentalnim vrednostima stepena konverzije TAG (srednje relativno procentno odstupanje između izračunatih i eksperimentalnih vrednosti *MRPD* = ±10,8%, na osnovu 81 podataka). Uprkos uporedivoj tačnosti, za opisivanje kinetike reakcije metanolize USK katalizovane negašenim krečom preporučuje se model koji uključuje promenljivi mehanizam reakcije i ograničenja prenosa mase TAG zbog jednostavnijeg proračuna i primenljivosti u celom toku reakcije.

Ključne reči: biodizel, ulje semena konoplje, metanoliza, kinetika, negašeni kreč.

CRediT authorship contribution statement:
Milan D. Kostić: Conceptualization, Methodology, Investigation, Visualization, Writing – Original Draft
Biljana S. Đorđević: Conceptualization, Methodology, Investigation, Visualization, Writing – Original Draft
Milica Z. Petković: Conceptualization, Methodology, Investigation, Visualization, Writing – Original Draft
Marija R. Miladinović: Validation, Writing – Original Draft, Writing – Reviewing and Editing
Olivera S. Stamenković: Validation, Writing – Original Draft, Writing – Reviewing and Editing